JOURNAL OF VIROLOGY, May 2006, p. 4691–4697 Vol. 80, No. 10
0022-538X/06/$08.00+0 doi:10.1128/JVI.80.10.4691–4697.2006

Effects of Mutations in the Human Immunodeficiency Virus Type 1 *gag* Gene on RNA Packaging and Recombination

Olga Nikolaitchik,[1] Terence D. Rhodes,[1] David Ott,[2] and Wei-Shau Hu[1]*

HIV Drug Resistance Program, National Cancer Institute,[1] and Basic Research Program, SAIC-Frederick,[2] Frederick, Maryland 21702

Received 6 January 2006/Accepted 28 February 2006

Human immunodeficiency virus type 1 (HIV-1) recombination occurs during reverse transcription when parts of the two copackaged RNAs are used as templates for DNA synthesis. It was previously hypothesized that HIV-1 Gag polyproteins preferentially encapsidate the RNA from which they were translated (*cis*-packaging hypothesis). This hypothesis implies that mutants encoding Gag that cannot efficiently package viral RNA are selected against at two levels: these mutants do not generate infectious virus, and these mutants are not efficiently rescued by the wild-type virus because the mutant RNAs are packaged at much lower levels than are those of the wild-type genome. Therefore, genetic information encoded by *gag* mutants can be rapidly lost in the viral population. To test this prediction of the *cis*-packaging hypothesis, we examined several *gag* mutants by measuring the efficiencies of the mutant RNAs in being packaged in *trans* in the presence of wild-type virus and determining the rates of recombination between *gag* mutants and wild-type viruses. We observed that the viral RNAs from the nucleocapsid zinc finger or the capsid truncation mutant were packaged efficiently in *trans*, and these mutant viruses also frequently recombined with the wild-type viruses. In contrast, viral RNAs from mutants containing a 6-nucleotide substitution encompassing the *gag* AUG were not efficiently encapsidated, resulting in a low rate of recombination between the mutants and wild-type viruses. Further analyses revealed that other, more subtle mutations changing the *gag* AUG and abolishing Gag translation did not interfere with efficient encapsidation of the mutant RNA. Our results indicated that neither the *gag* AUG sequence nor Gag translation is essential for viral RNA encapsidation, and Gag can package both wild-type and *gag* mutant RNAs with similar efficiencies. Therefore, we propose that HIV-1 RNA encapsidation occurs mainly in *trans*, and most *gag* mutants can be rescued by wild-type virus; therefore, they are unlikely to face the aforementioned double-negative selection.

The full-length retroviral genomic RNA is selectively encapsidated into virions through interactions between RNA and the Gag polyproteins (15, 20, 38). Human immunodeficiency virus type 1 (HIV-1) Gag polyproteins contain multiple domains that are cleaved into mature proteins soon after or during virus assembly; these domains include matrix (MA), capsid (CA), p2, nucleocapsid (NC), p1, and p6 (15, 20, 38, 39). As in many other retroviruses, the NC domain of HIV-1 Gag plays an important role in RNA recognition; mutations in NC can abolish the specific packaging of the viral RNA (4, 18, 19, 42). Full-length HIV-1 RNA contains elements important for RNA packaging; deletions or mutations of these elements could cause severe defects in the specific packaging of the virion RNA (1, 2, 7–10, 21, 28, 29, 41). Many of these RNA elements are located near the 5′ end of the viral RNA, which is highly structured and conserved among different HIV-1 isolates (31).

Although it is clear that Gag-RNA interaction is critical for the encapsidation of virion RNA, many details of the mechanisms of RNA packaging are currently unknown. Experimental evidence suggests that the same pool of HIV-1 full-length RNAs is used as the template for Gag/Gag-Pol translation and as genetic material for encapsidation into virus particles (6, 13). It is unclear where, when, and how Gag selects viral RNA for encapsidation. The *cis*-packaging hypothesis proposes that the newly synthesized Gag polyproteins preferentially bind to the RNA from which they have been translated and incorporate these RNAs into virions (34). From multiple studies, it is clear that HIV-1 Gag is capable of packaging viral RNA in *trans*, because HIV-1 vectors devoid of full-length *gag* can be packaged and undergo one round of viral replication when supplemented with viral proteins. However, the efficiency of the *trans*-packaging events is unknown, because most HIV-1 vectors cannot reach the same titers as those of the wild-type viruses (3). Several studies have compared relative packaging efficiencies of vectors with wild-type or mutant *gag* genes with conflicting results. Although some studies demonstrated a strong preference for packaging RNA in *cis* (27, 34), others did not show significant differences between the efficiencies of wild-type and *gag* mutant RNA packaging (28).

Packaging of two genetically different RNAs into the same virion (heterozygous virion formation) is a prerequisite for observable HIV-1 recombination events (22, 35). Recombination occurs during reverse transcription of the viral RNA into DNA when reverse transcriptase (RT) switches between two copackaged RNAs to generate a DNA copy containing a portion of the genetic information from each of the parental RNAs (12, 22, 23). Frequent HIV-1 recombination assorts the mutations generated during reverse transcription and increases the diversity of the viral population (11).

We are interested in determining the factors that can affect HIV-1 recombination rates and selection pressure on the various mutants. Whether HIV-1 Gag polyproteins preferentially package viral RNA in *cis* has important implications for the

* Corresponding author. Mailing address: HIV Drug Resistance Program, NCI-Frederick, P.O. Box B, Building 535, Room 336, Frederick, MD 21702. Phone: (301) 846-1250. Fax: (301) 846-6013. E-mail: whu@ncifcrf.gov.

selective pressure on *gag* mutants. The *cis*-packaging hypothesis implies that mutants that cannot generate functional Gag are selected against at two levels: these mutants do not generate infectious virus, and these mutant RNAs cannot efficiently compete with wild-type viral RNA for packaging. The packaging of mutant RNA allows the occurrence of recombination to preserve genetic information elsewhere in the genome. Therefore, the *cis*-packaging hypothesis predicts that the aforementioned *gag* mutants will be rapidly lost in the viral population.

To determine the mode of Gag-RNA interaction and to test the prediction of the *cis*-packaging hypothesis, we examined the abilities of *gag* mutant RNAs to be packaged in the presence of viruses containing wild-type *gag*. Additionally, we examined the abilities of these *gag* mutants to recombine with viruses encoding wild-type *gag*. Our results indicate that *gag* mutant RNAs can be packaged efficiently by Gag expressed in *trans*, and the ability to translate Gag is not a prerequisite for efficient encapsidation of the viral RNA, even in the presence of competing wild-type RNA. Furthermore, *gag* mutants can recombine frequently with wild-type viruses, indicating that *gag* mutants should not encounter more negative selection than do mutants of other viral genes.

MATERIALS AND METHODS

Plasmid construction. Standard molecular cloning techniques were used to construct plasmids (37). The names of all plasmids used in this study begin with "p"; the names of the viruses derived from these plasmids do not. For clarity, the previously described plasmids pON-H0 and pON-T6 (35) are referred to as pH0 and pT6, respectively. Plasmid pH0-Xba was derived from pH0; mutations near the AUG were introduced by replacing the StuI-to-SphI DNA fragment with that from pNLX (34). Plasmids pH0-Null and pH0-Spe were derived from pH0-Xba and pH0, respectively, by filling in the SpeI site in *gag* using the Klenow fragment of DNA polymerase I. This procedure simultaneously introduced a frameshift and an in-frame stop codon at residue 99 of CA. Plasmid pH0-NC was generated by replacing the SphI-to-SbfI fragment in pH0 with that of pNL43 CCCC/CCCC (pRB73) (19).

To generate pH0-ATGG, pH0-ATA, and pH0-AAG, PCR fragments containing the desired mutations were digested with SfoI and SpeI. These digested fragments were used to replace the equivalent fragments in pH0-SA, which is identical to pH0-Xba except that an SfoI site in the plasmid backbone was eliminated by fill-in reaction. The general structures of all constructs were verified by restriction enzyme mapping; all *gag* mutations and DNA fragments that had undergone PCR were characterized by DNA sequencing to avoid inadvertent mutations.

Cell culture, DNA transfection, virus infection, cell sorting, and flow cytometry analyses. Human embryonic kidney cell line 293T (14) and human T-cell line Hut/CCR5 (40) were maintained in Dulbecco's modified Eagle's medium and Roswell Park Memorial Institute-1640 medium, respectively. Both media were supplemented with 10% fetal calf serum, penicillin (50 U/ml), and streptomycin (50 U/ml). Puromycin (1 μg/ml) and G418 (500 μg/ml) were also added to the medium used for Hut/CCR5 cells. All cultured cells were maintained in humidified 37°C incubators with 5% CO_2.

DNA transfection was performed by the standard calcium phosphate method (37). Viral supernatant was harvested 48 h posttransfection, clarified through a 0.45-μm-pore-size filter to remove cellular debris, and used immediately or stored at −80°C prior to infection. Virus infection was performed in the presence of Polybrene at a final concentration of 50 μg/ml. Cells were processed and analyzed by flow cytometry 48 h (293T) to 72 h (Hut/CCR5) postinfection. To identify marker expression, cells were stained with phycoerythrin-conjugated anti-heat-stable antigen (anti-HSA) antibody (Becton Dickinson Biosciences, San Jose, CA) and allophycocyanin-conjugated anti-Thy1.2 antibody (eBioscience, San Diego, CA). Flow cytometry analyses were performed on a FACSCalibur system (Becton Dickinson Biosciences, San Jose, CA), and the data obtained were analyzed using the FlowJo software (Tree Star, Ashland, OR). As previously described (35), the two parental viruses were introduced into 293T cells by sequential infection at a low multiplicity of infection (MOI) of less than 0.1 (see Fig. 1D). Dually infected cells were enriched by cell sorting so that more than 93% of the cells expressed markers encoded by both vectors. Cell sorting was performed on a FACSVantage SE System with the FACSDiVa Digital Option (BD Biosciences).

Virion and cellular RNA isolation and analyses. Total cellular RNA was isolated using the Bio-Rad AquaPure RNA isolation kit according to the manufacturer's instructions. Cytoplasmic RNA was isolated from the producer cells using a standard protocol (17). Briefly, cells were collected by centrifugation and resuspended in lysis buffer; nuclei and cell debris were removed by centrifugation. The supernatant was treated with proteinase K, extracted with phenol-chloroform, and precipitated by ethanol. Virion RNA was isolated using a standard protocol (16). Briefly, clarified cell-free viral supernatant was concentrated by centrifugation at 25,000 rpm for 90 min at 4°C using a Surespin 630 (Sorvall) rotor and a Discovery 100S Sorvall ultracentrifuge. The virion-containing pellet was resuspended and treated with RNase-free DNase and proteinase K. Guanidinium isothiocyanate, glycogen, and isopropanol were added to precipitate the RNA. All RNA samples were resuspended in RNase-free water and stored at −80°C.

The RT-PCR sequencing technique was used to determine the ratio of wild-type and mutant viral RNAs in various samples (25). Titration with known ratios of wild-type and mutant plasmids was performed to ensure the accuracy of the method. RNA samples were treated with DNase I prior to RT-PCR, which was performed using the SuperScript One-Step RT-PCR with Platinum *Taq* kit (Invitrogen, Carlsbad, CA). For each RNA sample, a control was performed to detect potential DNA contamination by conducting the PCR without the RT step. Gel-eluted RT-PCR products were sequenced. RT-PCR amplified both wild-type and mutant RNAs, and the polymorphism of the two templates was revealed in the DNA sequencing chromatogram. The relative amounts of the two templates were quantified by analyzing the relative heights of the peaks of the discordant signal in the chromatogram.

Allele-specific real-time PCR was performed to verify the RT-PCR sequencing data in some samples (33). For the allele-specific real-time PCR, viral RNA was first copied to DNA and then amplified by PCR. The amount of the amplified DNA was quantified using SYBR green fluorescence, and the specificity of the amplification was confirmed by a melting-curve analysis of the PCR product. These DNAs were then subjected to a second round of real-time PCR using discriminating primer sets with appropriate standard curves. The numbers from both mutant and wild-type analyses were combined and adjusted to a total of 100%. All analyses were done in triplicate, and at least two sets of independent samples were examined.

RESULTS

Experimental strategy used to test the prediction of the *cis*-packaging hypothesis. One of the predictions of the *cis*-packaging hypothesis is that RNAs from certain HIV-1 *gag* mutants will be inefficiently packaged in the presence of wild-type RNA from which functional Gag can be translated. Furthermore, this deficiency in RNA packaging will result in a severe reduction in the ability of these *gag* mutants to recombine with HIV-1 encoding wild-type Gag. To test this prediction of the *cis*-packaging hypothesis, we measured the ability of *gag* mutants to be propagated in the presence of wild-type Gag and measured the rates of recombination between an HIV-1 vector containing wild-type *gag* and an HIV-1 vector with mutant *gag*.

The structures of vectors used in this study are shown in Fig. 1. All of these NL4-3-based vectors contain *cis*-acting elements essential for virus replication, *gag-pol*, *tat*, and *rev*, and have deletion mutations in *vif*, *vpu*, *vpr*, and *env*. Additionally, each vector carries two marker genes placed in the *nef* reading frame: the first marker gene is either a mouse heat-stable antigen gene (*hsa*) or a mouse CD90.2 gene (*thy*); the second marker gene is a green fluorescent protein (GFP) gene (*gfp*). Vector pH0 contains a functional *hsa* gene and a nonfunctional *gfp* gene with an inactivating mutation 16 nucleotides (nt) downstream of the start codon of *gfp*. Vector pT6 contains a functional *thy* gene and a nonfunctional *gfp* gene with an inactivating mutation 603 nt

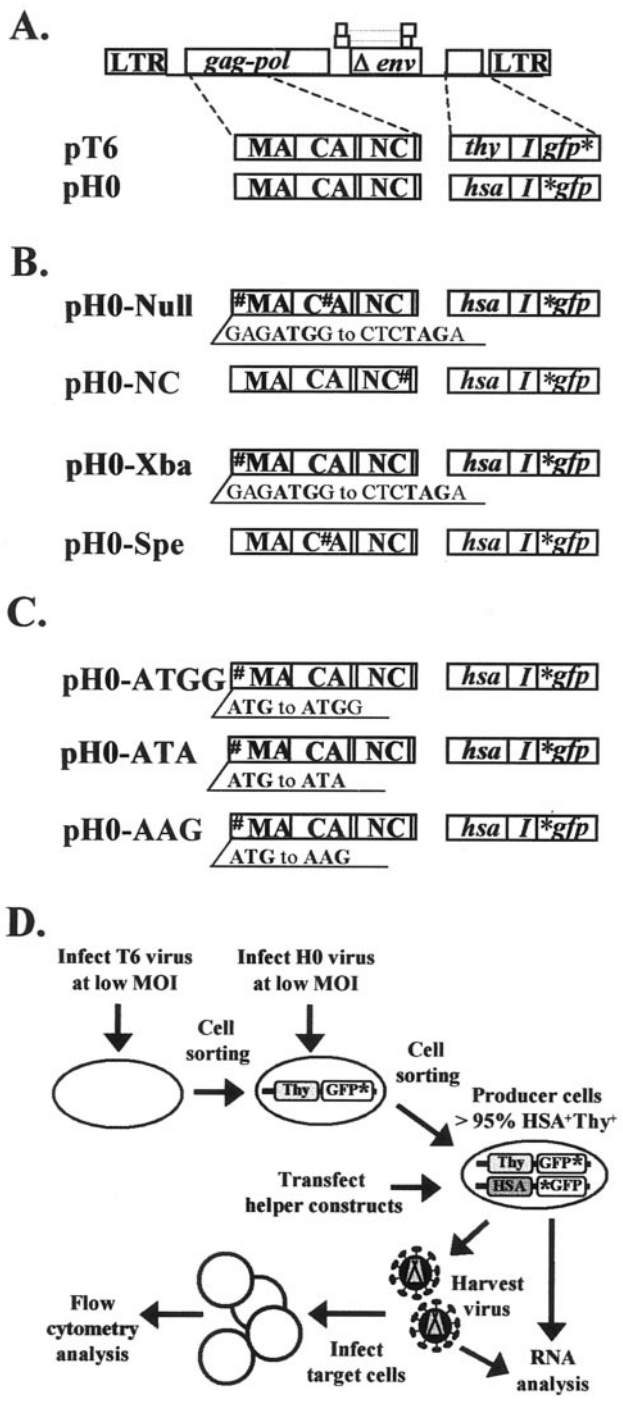

FIG. 1. (A to C) General structures of the vectors and experimental protocol used to test the effects of *gag* mutations on RNA packaging and recombination: vectors containing wild-type *gag* genes (A), previously described mutant *gag* genes (B), or *gag* genes with start codon mutations (C). (D) Outline of the experimental protocol. Plasmid pT6 has the same structure as pH0 except for the marker genes that are carried. All other vectors have structures identical to that of pH0 except for the mutations introduced in *gag* genes; nucleotide sequences under the vector structures indicate the sequence alterations. The start codon of *gag* is indicated in boldface; the inactivating mutations in *gfp* are indicated by asterisks, whereas the mutations in *gag* are indicated by number signs; I, internal ribosome entry site.

downstream from the start codon of *gfp*. The distance between the two inactivating mutations is 588 nt.

We used a previously established system (35) to examine the replication of *gag* mutants in the presence of wild-type vector and recombination between a *gag* mutant and a wild-type vector. The experimental protocol is outlined in Fig. 1D. Vector plasmids were transfected into 293T cells along with helper plasmids pCMVΔ8.2 (30) and pHCMVG (5), which express HIV-1 proteins and the G protein from vesicular stomatitis virus, respectively. Viruses generated from this process were used to sequentially infect 293T cells at a low MOI to avoid the presence of multiple proviruses in each cell. Dually infected cells were enriched by cell sorting so that more than 93% of the cells in each producer cell line expressed both HSA and Thy. To examine virus replication and recombination, the producer cell line was transfected with pIIINL(AD8)env, which expresses CCR5-tropic HIV-1 Env, and helper plasmid pCMV-dGag (35), which expresses all of the HIV-1 accessory genes. Viruses were harvested 48 h posttransfection and were used to infect target Hut78/CCR5 T cells; these cells were processed and analyzed by flow cytometry 72 h postinfection.

In this system, flow cytometry analyses measure the titers of the two parental viruses and the recombinant. Infection by the T6 or H0 vector is monitored by the numbers of cells expressing Thy (Thy^+) or HSA (HSA^+), respectively. Although both H0 and T6 vectors contain mutant *gfp*, a functional *gfp* could be generated by recombination during reverse transcription of the heterozygous viruses containing T6 and H0 RNAs. Therefore, the numbers of cells expressing GFP (GFP^+) can be used to measure recombination events. As previously described (35), the numbers of infected cells were converted into MOI, and the recombination rate was calculated by dividing the GFP MOI by the overall-infection MOI.

Replication and recombination between a vector with wild-type *gag* and vectors with mutant *gag*. To examine the effects of *gag* mutation on replication assisted by *trans*-acting proteins and recombination, we constructed two derivatives of pH0, pH0-Null and pH0-NC, each containing a previously described *gag* mutation (Fig. 1). Vector pH0-Null has the same mutations in *gag* as does pNLXX (34)—namely, a 6-nt substitution to abolish the AUG start codon of *gag* and a 4-nt insertion in the CA domain of *gag* that introduces a +1 frameshift and a stop codon. These two mutations eliminate the translation of full-length Gag from the authentic start site and truncate the translation of the internally initiated partial Gag termed Gag* (34). Vector pH0-NC altered both zinc finger motifs from CCHC to CCCC; this mutation has been shown to cause significant loss of viral RNA packaging specificity (less than 5% viral RNA compared with wild-type virions) and a severe reduction in their infectivity (19). The phenotypes of both pH0-Null and pH0-NC were confirmed by various methods including Western analyses, virus infection, and flow cytometry (data not shown).

We generated producer cell lines containing the T6 provirus plus either the H0-Null or H0-NC provirus and performed the aforementioned replication and recombination assay; the results of these experiments are shown in Fig. 2. Previously, we reported that the rate of recombination of H0 and T6, both containing wild-type *gag*, was approximately 7% (i.e., approximately 7% of the infection events led to the GFP^+ pheno-

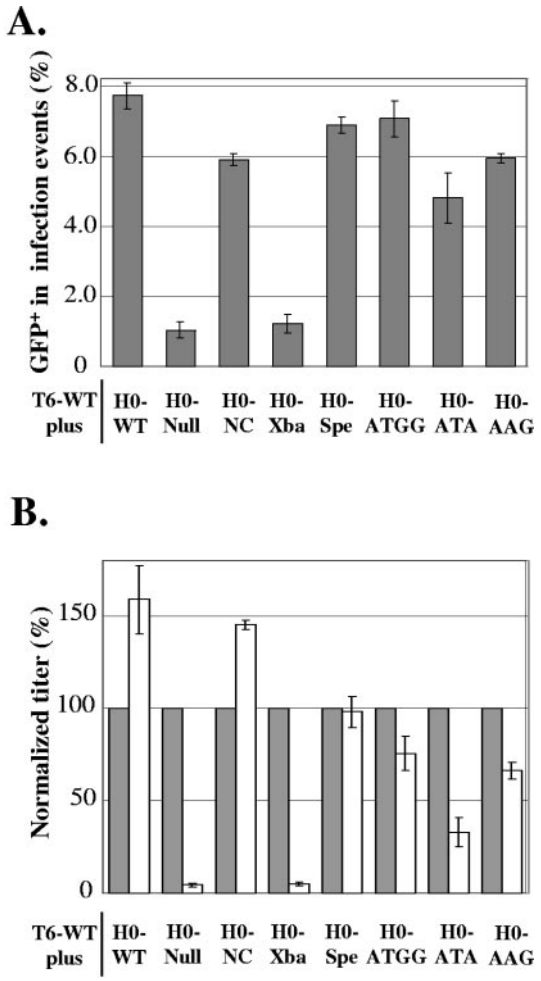

FIG. 2. Effects of *gag* mutations on the abilities of the mutant vectors to be rescued by and to recombine with a wild-type vector. (A) Rates of recombination between vectors with wild-type *gag* and those with mutant *gag*. The *y* axis denotes the percentage of infection events that reconstitute the GFP^+ phenotype. (B) Relative titers of the wild-type viruses and the *gag* mutants in one round of virus replication. Gray bars represent wild-type virus titers, which were set to 100%; white bars represent *gag* mutant titers, which were normalized to the wild-type vector titers. The results from at least two independent experiments are summarized; error bars indicate standard deviations. WT, wild type.

type). The recombination rate generated by T6 and H0-Null was 1.1% ± 0.2%, which was approximately seven times lower than that of the wild-type H0 and T6 (Fig. 2A). However, the recombination rate generated by T6 and H0-NC was 5.9% ± 0.2%, which was close to that of H0 and T6 (Fig. 2A).

We have also determined the viral titers from *gag* mutants and wild-type T6 by measuring the numbers of HSA- and Thy-expressing target cells, respectively. Viral titers generated from producer cells expressing both T6 and H0-Null indicated that the H0-Null titers were severely reduced compared with the T6 titers. In contrast, viruses from producer cells expressing T6 and H0-NC generated similar T6 and H0-NC titers (Fig. 2B). These results indicate that, although both H0-Null and H0-NC contained mutations in *gag*, these two mutants had very different properties. The titers of H0-NC were similar to those of T6, indicating that, although the mutant Gag expressed by H0-NC could not specifically package viral RNA, RNA derived from H0-NC could be encapsidated efficiently by the wild-type Gag generated by T6. Therefore, HIV-1 Gag can package RNA in *trans* in a very efficient manner.

These titer data also revealed the possible reason behind the observed lower rate of recombination between H0-Null and T6. It is likely that, compared with T6 RNA, H0-Null RNA was not packaged efficiently; this defect decreased both the H0-Null titer and heterozygous virion formation, thereby lowering the rate of recombination between T6 and H0-Null. To understand why H0-Null and H0-NC exhibited such different properties, we further examined the mutations in H0-Null that may have caused its phenotype.

Dissecting the mutation that caused the H0-Null phenotype. Vector pH0-Null contains two mutations in *gag*. To determine whether one or both mutations caused the H0-Null phenotype, we constructed two vectors, each containing only one of the mutations: pH0-Xba contains the 6-nt substitution near the *gag* start codon, and pH0-Spe contains the 4-nt insertion in CA (Fig. 1). We generated producer cells containing the wild-type T6 vector and either the H0-Xba or H0-Spe vector and measured viral titers and recombination rates in one round of replication. The rate of recombination between T6 and H0-Xba was 1.2% ± 0.3%, which was much lower than that of two wild-type vectors and similar to that of T6 and H0-Null (Fig. 2A). In contrast, the rate of recombination between T6 and H0-Spe was 6.9% ± 0.2%, similar to the rate of two wild-type vectors (Fig. 2A). Analyses of the viral titers indicated that H0-Xba generated much lower viral titers than did T6, whereas H0-Spe generated titers similar to those of T6. These results demonstrated that the H0-Null phenotype was caused by the mutations around the *gag* AUG start codon.

The four mutants that we examined thus far can be divided into two groups. H0-Null and H0-Xba generated virus titers far lower than those of T6 and recombined with the T6 vector at a low frequency. In contrast, H0-NC and H0-Spe generated viral titers similar to those of the wild-type vector T6 and recombined with T6 at high frequencies. These results suggested that the differences between these two phenotypes are caused by the efficiencies of viral RNA packaging. To test this possibility, we quantified the amounts of viral RNAs in the producer cells and cell-free virions.

Analyses of viral RNA in producer cells and cell-free virions. To determine the efficiency of the viral RNA packaging, we isolated cytoplasmic RNA from the producer cells and RNA from cell-free supernatants and analyzed these samples by RT-PCR sequencing. Using primers annealed specifically to the unspliced, full-length viral RNAs, we used RT-PCR to amplify a portion of the viral genome containing the region that is different between T6 and *gag* mutants and sequenced these PCR products. RT-PCR amplified both T6 and *gag* mutant RNAs; during the sequencing reaction, the polymorphism of the input templates generated two different DNA sequencing signals at or beyond the mutation. The relative amounts of the two vectors in the PCR product were reflected in the sequencing chromatogram, which could be quantified by analyzing the relative height of the peaks of the discordant signals. The RT-PCR sequencing approach has been used by others to quantify relative amounts of RNAs in a given sample (25). We

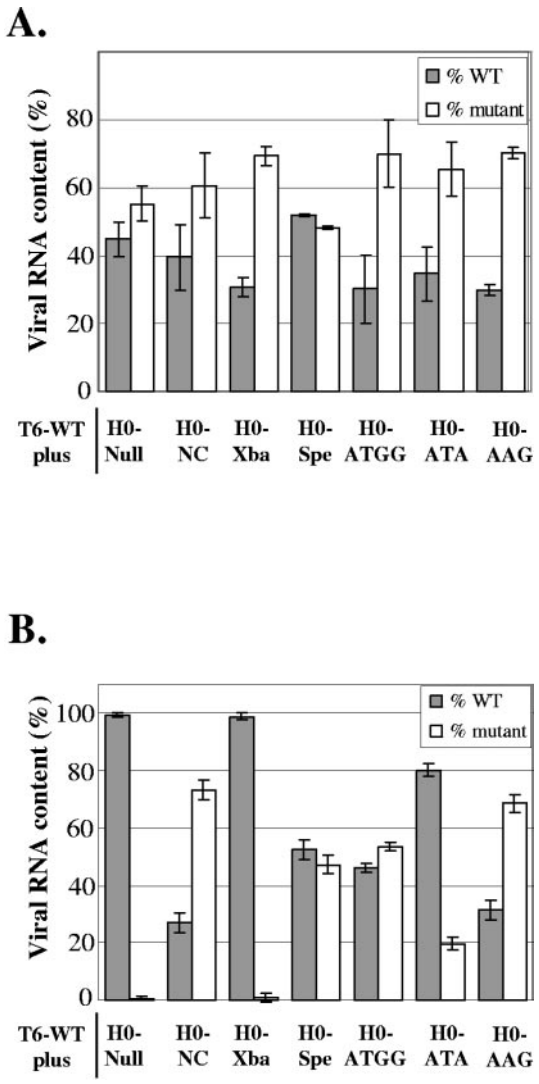

FIG. 3. Packaging efficiencies of the wild-type and *gag* mutant viral RNAs. The ratios of wild-type and mutant viral RNAs in the cytoplasm of the producer cells (A) and in cell-free virions (B) are shown. In each sample, the total viral RNA was set to 100%; wild-type viral RNAs (gray bars) or *gag* mutant viral RNAs (white bars) are shown as a percentage of the total viral RNA. The results from at least two independent experiments are summarized; error bars indicate standard deviations. WT, wild type.

have also performed this assay with various known amounts of input DNAs and found that this method can reliably detect mixtures of templates at ratios from 1:1 to 1:10 (data not shown).

The relative amounts of T6 and *gag* mutant RNA in the cytoplasm of the producer cells are summarized in Fig. 3A. We found that in the producer cells RNAs from the aforementioned four *gag* mutants were present at levels similar to those of T6 RNA. Therefore, the low viral titers generated by H0-Null and H0-Xba were not caused by the lack of full-length *gag* mutant RNA in the cytoplasm of the cells.

We then examined the RNAs from virions generated by producer cells and observed that H0-NC and H0-Spe RNAs were packaged efficiently (Fig. 3B). In contrast, H0-Null and H0-Xba RNAs were packaged at severely reduced levels (Fig. 3B). The RT-PCR sequencing method has limited detection sensitivity when the two RNA species are present at very different proportions; therefore, we confirmed our results with allele-specific real time RT-PCR (33). Using controls with defined mixtures of T6 and *gag* mutant templates, we were able to detect a minor species of RNA at the level of 0.1% of the total content (data not shown). Allele-specific PCR analyses of the virion RNAs indicated that H0-Null and H0-Xba RNAs were packaged at severely reduced levels: 1.7% ± 0.4% and 3.2% ± 0.5%, respectively, of the total viral RNA content. Therefore, H0-Null and H0-Xba RNAs were packaged approximately 20- to 30-fold less efficiently than expected based on the level of mutant RNAs in the producer cells.

Together, our findings indicate that the RNAs of all four mutants were expressed in abundant levels in the producer cells but packaged at different efficiencies. H0-NC and H0-Spe RNAs could be packaged efficiently, whereas H0-Null and H0-Xba RNAs had a severe packaging defect.

Effects of active Gag translation on viral RNA packaging. Our data presented so far did not shed light on the possible mechanism(s) that caused the packaging defects of H0-Null and H0-Xba. Translation of Gag using the authentic AUG codon occurred in both H0-NC and H0-Spe but not in H0-Null and H0-Xba. H0-Null and H0-Xba shared the same mutation that destroyed *gag* AUG. The packaging defects in these two viruses could have been caused by the inability to initiate translation at the *gag* AUG codon or the disruption of the *cis*-acting packaging signals. To distinguish between these two mechanisms, we generated three additional mutants containing mutations at the AUG site. In vectors H0-ATA and H0-AAG, the *gag* AUG start codon was changed to AUA and AAG, respectively. In vector H0-ATGG, a G was inserted after AUG to generate a +1 frameshift in the *gag* reading frame, which could be translated to generate a 13-amino-acid peptide. If the ability to initiate Gag translation at the authentic AUG site is critical to RNA packaging, then both H0-ATA and H0-AAG would have packaging defects. If the mutations in H0-Null and H0-Xba affected *cis*-acting elements, then it is possible that some of the three mutants would not exhibit packaging defects.

We generated producer cell lines containing T6 and one of the AUG mutants and analyzed viral titers, recombination rates, and RNA packaging efficiencies. We found that H0-ATGG and H0-AAG both were expressed well in producer cells (Fig. 3A), and their RNAs were packaged efficiently into virions (Fig. 3B). Furthermore, these two vectors had high viral titers (Fig. 2B), and recombined frequently with T6 at the same level as that of the two wild-type vectors (Fig. 2A).

Vector H0-ATA was also expressed well in the producer cells (Fig. 3A); however, this vector had a very mild packaging defect as shown by the slight decrease of the mutant RNA packaged in virions (Fig. 3B), the viral titer (Fig. 2B), and the recombination rate (Fig. 2A) compared with those of the other two AUG mutants.

Taken together, our results indicate that active translation or the initiation of Gag translation at the authentic AUG codon is not necessary for efficient viral RNA packaging. Our results suggest that the mutation in H0-Null and H0-Xba caused the

packaging defect, probably by disrupting *cis*-acting elements important for viral RNA packaging.

DISCUSSION

In this report, we have examined the efficiencies of RNAs from *gag* mutants in being packaged in *trans* into HIV-1 virions. We observed that, in the presence of viral RNA from which wild-type Gag was translated, RNAs from several *gag* mutants were packaged and propagated very efficiently. These mutants include an NC mutant with packaging-defective Gag, a CA truncation mutant, and three mutants in which the *gag* start codon was abolished. Therefore, translation of the functional Gag or translation from the authentic *gag* start codon is not required for RNA encapsidation. Taken together, our results indicate that *trans*-packaging is a major mechanism of HIV-1 RNA encapsidation.

It was previously reported that the RNA from vector pNLXX, which contained the same *gag* mutations as those in H0-Null, was packaged at an eightfold-reduced efficiency compared with the wild-type vector (34). Based on this result and other data, it was proposed that HIV-1 Gag preferentially packages RNA in *cis*. In our study, we also observed a significant defect in RNA packaging of this mutant, approximately a 30-fold decrease in RNA encapsidation. However, because other *gag* mutants were packaged efficiently, we conclude that *cis* packaging did not cause the encapsidation defect in the H0-Null mutant.

Both H0-Null and H0-Xba have the 6-nt substitutions eliminating the *gag* AUG codon, and their RNAs have packaging defects. It was previously suggested that abolishing AUG could cause rapid degradation of full-length RNA from Rous sarcoma virus (24). Our cellular RNA analyses concurred with the previous work (34) and indicated that there are abundant amounts of mutant RNA; hence, rapid degradation did not cause the lack of encapsidated mutant RNA.

Most of the known *cis*-acting elements important for HIV-1 RNA encapsidation reside at the first 1,500 nt of the HIV-1 genome (26, 32, 36). Several folding models for the 5′ region of the HIV-1 RNA genome were proposed over the years; a major model postulated that the region from the primer binding site to the 5′ end of *gag* is folded into four stem loops termed SL1 to SL4 (8). Another model proposed that the 5′ region of HIV-1 RNA exists in two alternative conformations, long-distance interaction (LDI) and branched multiple hairpin (BMH), that are in dynamic equilibrium. It was proposed that LDI RNA is favored for translation, whereas BMH RNA is favored for dimerization and encapsidation (1, 2, 31).

One possible explanation for the packaging defect caused by the 6-nt substitution is that these mutations caused the equilibrium of the RNA to shift toward LDI, and LDI RNA is proposed not to be a good substrate for RNA packaging. The 6-nt substitution disrupted 5 of the 10 paired bases between U5 and the sequences near the *gag* AUG codon (U5-AUG duplex) that are critical to maintaining the proposed BMH conformation (2) and only two of the seven paired bases in proposed LDI conformation. Consistent with this possibility, the predicted RNA folding indicated that the other three AUG mutants minimally disrupted the base pairing of the U5-AUG duplex (data not shown), and we did not observe severe packaging defects in these mutants. Alternatively, it is also possible that the 6-nt substitution distorted the RNA folding and disrupted the RNA structure(s) important for the Gag-RNA interaction, thereby causing the packaging defect of the H0-Null mutant RNA.

In this report, we have examined several mutants that could not express functional Gag proteins capable of packaging viral RNA. We found that RNAs from most of the *gag* mutants could be efficiently packaged into virions and rescued by protein expressed in *trans*. Furthermore, recombination occurred frequently between the *gag* mutant and the wild-type virus, indicating that the genetic information elsewhere in these *gag* mutants could still be preserved in the viral population. Therefore, the negative selective pressure for *gag* mutants is likely to be similar to that for viruses harboring mutations in other genes such as *pol* or *env*. Barring the dominant-negative mutants, viruses with debilitating mutations in their coding regions can still serve as part of the genetic reservoir in the viral population.

ACKNOWLEDGMENTS

We thank Anne Arthur for her expert editorial help; Vinay K. Pathak for intellectual input throughout the project; John Coffin for advice on the appropriate methods of RNA analyses; Robert Gorelick and Vinay K. Pathak for critical reading of the manuscript; and Valerie Boltz, Sarah Palmer, and John Coffin for their help with the allele-specific RT-PCR.

This research was supported in part by the Intramural Research Program of the NIH, National Cancer Institute, Center for Cancer Research, and in part by NCI contract no. N01-CO-12400.

REFERENCES

1. **Abbink, T. E., and B. Berkhout.** 2003. A novel long distance base-pairing interaction in human immunodeficiency virus type 1 RNA occludes the Gag start codon. J. Biol. Chem. **278:**11601–11611.
2. **Abbink, T. E., M. Ooms, P. C. Haasnoot, and B. Berkhout.** 2005. The HIV-1 leader RNA conformational switch regulates RNA dimerization but does not regulate mRNA translation. Biochemistry **44:**9058–9066.
3. **Barker, E., and V. Planelles.** 2003. Vectors derived from the human immunodeficiency virus, HIV-1. Front. Biosci. **8:**d491–d510.
4. **Berkowitz, R. D., A. Ohagen, S. Hoglund, and S. P. Goff.** 1995. Retroviral nucleocapsid domains mediate the specific recognition of genomic viral RNAs by chimeric Gag polyproteins during RNA packaging in vivo. J. Virol. **69:**6445–6456.
5. **Burns, J. C., T. Friedmann, W. Driever, M. Burrascano, and J. K. Yee.** 1993. Vesicular stomatitis virus G glycoprotein pseudotyped retroviral vectors: concentration to very high titer and efficient gene transfer into mammalian and nonmammalian cells. Proc. Natl. Acad. Sci. USA **90:**8033–8037.
6. **Butsch, M., and K. Boris-Lawrie.** 2000. Translation is not required to generate virion precursor RNA in human immunodeficiency virus type 1-infected T cells. J. Virol. **74:**11531–11537.
7. **Clever, J., C. Sassetti, and T. G. Parslow.** 1995. RNA secondary structure and binding sites for gag gene products in the 5′ packaging signal of human immunodeficiency virus type 1. J. Virol. **69:**2101–2109.
8. **Clever, J. L., D. Mirandar, Jr., and T. G. Parslow.** 2002. RNA structure and packaging signals in the 5′ leader region of the human immunodeficiency virus type 1 genome. J. Virol. **76:**12381–12387.
9. **Clever, J. L., and T. G. Parslow.** 1997. Mutant human immunodeficiency virus type 1 genomes with defects in RNA dimerization or encapsidation. J. Virol. **71:**3407–3414.
10. **Clever, J. L., M. L. Wong, and T. G. Parslow.** 1996. Requirements for kissing-loop-mediated dimerization of human immunodeficiency virus RNA. J. Virol. **70:**5902–5908.
11. **Coffin, J. M.** 1995. HIV population dynamics in vivo: implications for genetic variation, pathogenesis, and therapy. Science **267:**483–489.
12. **Coffin, J. M.** 1979. Structure, replication, and recombination of retrovirus genomes: some unifying hypotheses. J. Gen. Virol. **42:**1–26.
13. **Dorman, N., and A. Lever.** 2000. Comparison of viral genomic RNA sorting mechanisms in human immunodeficiency virus type 1 (HIV-1), HIV-2, and Moloney murine leukemia virus. J. Virol. **74:**11413–11417.
14. **DuBridge, R. B., P. Tang, H. C. Hsia, P. M. Leong, J. H. Miller, and M. P. Calos.** 1987. Analysis of mutation in human cells by using an Epstein-Barr virus shuttle system. Mol. Cell. Biol. **7:**379–387.

15. **Freed, E. O.** 1998. HIV-1 gag proteins: diverse functions in the virus life cycle. Virology **251:**1–15.
16. **Fu, W., R. J. Gorelick, and A. Rein.** 1994. Characterization of human immunodeficiency virus type 1 dimeric RNA from wild-type and protease-defective virions. J. Virol. **68:**5013–5018.
17. **Gilman, M.** 2000. Preparation of RNA from eukaryotic and prokaryotic cells, p. 4.1.2–4.1.6. *In* F. M. Ausubel, R. Brent, R. E. Kingston, D. D. Moore, J. G. Seidman, J. A. Smith, and K. Struhl (ed.), Current protocols in molecular biology. John Wiley and Sons, Inc., Hoboken, N.J.
18. **Gorelick, R. J., D. J. Chabot, A. Rein, L. E. Henderson, and L. O. Arthur.** 1993. The two zinc fingers in the human immunodeficiency virus type 1 nucleocapsid protein are not functionally equivalent. J. Virol. **67:**4027–4036.
19. **Gorelick, R. J., T. D. Gagliardi, W. J. Bosche, T. A. Wiltrout, L. V. Coren, D. J. Chabot, J. D. Lifson, L. E. Henderson, and L. O. Arthur.** 1999. Strict conservation of the retroviral nucleocapsid protein zinc finger is strongly influenced by its role in viral infection processes: characterization of HIV-1 particles containing mutant nucleocapsid zinc-coordinating sequences. Virology **256:**92–104.
20. **Gottlinger, H. G.** 2001. The HIV-1 assembly machine. AIDS **15**(Suppl. 5)**:**S13–S20.
21. **Helga-Maria, C., M. L. Hammarskjold, and D. Rekosh.** 1999. An intact TAR element and cytoplasmic localization are necessary for efficient packaging of human immunodeficiency virus type 1 genomic RNA. J. Virol. **73:**4127–4135.
22. **Hu, W. S., and H. M. Temin.** 1990. Genetic consequences of packaging two RNA genomes in one retroviral particle: pseudodiploidy and high rate of genetic recombination. Proc. Natl. Acad. Sci. USA **87:**1556–1560.
23. **Hwang, C. K., E. S. Svarovskaia, and V. K. Pathak.** 2001. Dynamic copy choice: steady state between murine leukemia virus polymerase and polymerase-dependent RNase H activity determines frequency of in vivo template switching. Proc. Natl. Acad. Sci. USA **98:**12209–12214.
24. **LeBlanc, J. J., and K. L. Beemon.** 2004. Unspliced Rous sarcoma virus genomic RNAs are translated and subjected to nonsense-mediated mRNA decay before packaging. J. Virol. **78:**5139–5146.
25. **Leitner, T., E. Halapi, G. Scarlatti, P. Rossi, J. Albert, E. M. Fenyo, and M. Uhlen.** 1993. Analysis of heterogeneous viral populations by direct DNA sequencing. BioTechniques **15:**120–127.
26. **Lever, A. M.** 2000. HIV RNA packaging and lentivirus-based vectors. Adv. Pharmacol. **48:**1–28.
27. **Liang, C., J. Hu, R. S. Russell, and M. A. Wainberg.** 2002. Translation of Pr55(gag) augments packaging of human immunodeficiency virus type 1 RNA in a cis-acting manner. AIDS Res. Hum. Retrovir. **18:**1117–1126.
28. **McBride, M. S., and A. T. Panganiban.** 1996. The human immunodeficiency virus type 1 encapsidation site is a multipartite RNA element composed of functional hairpin structures. J. Virol. **70:**2963–2973.
29. **McBride, M. S., and A. T. Panganiban.** 1997. Position dependence of functional hairpins important for human immunodeficiency virus type 1 RNA encapsidation in vivo. J. Virol. **71:**2050–2058.
30. **Naldini, L., U. Blomer, P. Gallay, D. Ory, R. Mulligan, F. H. Gage, I. M. Verma, and D. Trono.** 1996. In vivo gene delivery and stable transduction of nondividing cells by a lentiviral vector. Science **272:**263–267.
31. **Ooms, M., H. Huthoff, R. Russell, C. Liang, and B. Berkhout.** 2004. A riboswitch regulates RNA dimerization and packaging in human immunodeficiency virus type 1 virions. J. Virol. **78:**10814–10819.
32. **Paillart, J. C., M. Shehu-Xhilaga, R. Marquet, and J. Mak.** 2004. Dimerization of retroviral RNA genomes: an inseparable pair. Nat Rev. Microbiol. **2:**461–472.
33. **Palmer, S., M. Kearney, F. Maldarelli, E. K. Halvas, C. J. Bixby, H. Bazmi, D. Rock, J. Falloon, R. T. Davey, Jr., R. L. Dewar, J. A. Metcalf, S. Hammer, J. W. Mellors, and J. M. Coffin.** 2005. Multiple, linked human immunodeficiency virus type 1 drug resistance mutations in treatment-experienced patients are missed by standard genotype analysis. J. Clin. Microbiol. **43:**406–413.
34. **Poon, D. T., E. N. Chertova, and D. E. Ott.** 2002. Human immunodeficiency virus type 1 preferentially encapsidates genomic RNAs that encode Pr55(Gag): functional linkage between translation and RNA packaging. Virology **293:**368–378.
35. **Rhodes, T. D., O. Nikolaitchik, J. Chen, D. Powell, and W. S. Hu.** 2005. Genetic recombination of human immunodeficiency virus type 1 in one round of viral replication: effects of genetic distance, target cells, accessory genes, and lack of high negative interference in crossover events. J. Virol. **79:**1666–1677.
36. **Russell, R. S., C. Liang, and M. A. Wainberg.** 2004. Is HIV-1 RNA dimerization a prerequisite for packaging? Yes, no, probably? Retrovirology **1:**23.
37. **Sambrook, J., E. F. Fritsch, and T. Maniatis.** 1989. Molecular cloning: a laboratory manual, 2nd ed. Cold Spring Harbor Laboratory Press, Cold Spring Harbor, N.Y.
38. **Swanstrom, R., and J. W. Wills.** 1997. Synthesis, assembly, and processing of viral proteins, p. 263–334. *In* J. M. Coffin, S. H. Hughes, and H. E. Varmus (ed.), Retroviruses. Cold Spring Harbor Laboratory Press, Cold Spring Harbor, N.Y.
39. **Vogt, V. M.** 1997. Retroviral virions and genomes. Cold Spring Harbor Laboratory Press, Cold Spring Harbor, N.Y.
40. **Wu, L., T. D. Martin, R. Vazeux, D. Unutmaz, and V. N. KewalRamani.** 2002. Functional evaluation of DC-SIGN monoclonal antibodies reveals DC-SIGN interactions with ICAM-3 do not promote human immunodeficiency virus type 1 transmission. J. Virol. **76:**5905–5914.
41. **Zeffman, A., S. Hassard, G. Varani, and A. Lever.** 2000. The major HIV-1 packaging signal is an extended bulged stem loop whose structure is altered on interaction with the Gag polyprotein. J. Mol. Biol. **297:**877–893.
42. **Zhang, Y., and E. Barklis.** 1997. Effects of nucleocapsid mutations on human immunodeficiency virus assembly and RNA encapsidation. J. Virol. **71:**6765–6776.